# SIMULATION OF A STEAM BUBBLE TRANSPORT IN THE PRIMARY SYSTEM OF THE POOL TYPE LEAD COOLED FAST REACTORS

**Marti Jeltsov and Pavel Kudinov**
Royal Institute of Technology, Stockholm, Sweden
marti@safety.sci.kth.se, pavel@safety.sci.kth.se

## Abstract

Pool-type design makes Lead cooled Fast Reactor (LFR) economically competitive with other advanced reactor designs considered under the Generation IV framework. However, close proximity of steam generator to the core increases the risks associated with Steam Generator Tube Rupture/Leakage (SGTR/SGTL) such as voiding of the core and resulting reactivity insertion and/or local damage (burnout) of fuel rod cladding. Analysis of consequences of SGTL provided in present paper suggests that small bubbles of steam can be dragged by the turbulent coolant flow into the core region. Trajectories of the bubbles are determined by location of the leak, bubbles size and turbulent flow field of lead coolant. The influence of epistemic uncertainty in drag coefficient on prediction of the fraction of bubbles that can reach the core and accumulate in the primary coolant system is discussed in the paper.

**Keywords:** Lead cooled systems, Steam Generator Tube Rupture/Leakage, bubble drag, core voiding, CFD

## Introduction

Lead and lead-alloy cooled fast reactor (LFR) systems constitute one of the six concepts of advanced reactor design considered for research and development under the Generation IV framework. Mission and criteria for development and operation of future fast reactors were discussed by Spencer [1], who provided a comprehensive review of various aspects of using lead coolant technology. A fine balance between economics and safety of LFR lies on assuring the feasibility of having the steam generator in the primary coolant circuit, thus eliminating the need for (and economic burden of) an intermediate circuit as such in sodium-cooled fast reactors.

Discussion of different safety concerns associated with close proximity of steam generator to the core in pool type LFR design can be found in [1] and [2]. SGTR/L can become a showstopper for licensing of LFR technology, given that potential direct consequences of SGTR/L are high (core damage) and frequency is uncertain due to the lack of operational experience. To assess the risk and provide adequate defence-in-depth for SGTR/L in LFR both frequency and consequences need to be clarified. Among the safety concerns described in [2] there is a potential for core voiding that might cause reactivity insertion and local fuel damage in case of small leak from a SG tube.

Leakage of SG tube is not a new safety issue per se. Significant efforts have been undertaken to changes in the design, coolant chemistry, and adjustment of frequencies of SG inspections, to keep under control the SGTR in pressurized water reactors (PWRs). Nevertheless, analysis of available statistics [2] for PWRs shows that there were 9 cases of SG tube rupture in US during 1975-2000 and about 40 cases of SG tube leak incidents during 9 years of 1990-1998. Comparing potential for occurrence of SGTR in PWR and in LFR it is important to mention that lead, as a coolant, has higher density and is very corrosive for the structural materials. These factors generally accelerate chemical and mechanical wearing and degradation of the steam generator tubings, thus increasing frequency of SGTR occurrence.

From the PWR operational experience and from experiments performed on degraded SG tubing (e.g. [3]) it is well known that a small leak usually precede a large rupture of the tube. The leak can last for many days. In fact, EPRI guidelines [4] recommend increased monitoring if leak exceeds 20 litres per day, and below that value no specific actions are recommended during normal operation of a PWR.

The main objective of the present study is to quantify the likelihood that a steam bubble is transported in the primary coolant system to the core in case of SG tube leakage. The ELSY (European Lead-Cooled SYstem) pool-type LFR 600 MWe [5] is used as a reference design (Figure 1). The core is submerged in the middle part of the pool and surrounded by 8 steam generators (SG), located at the top part of the pool. A coaxial pump is installed inside each SG. The SG in lead-cooled systems provides active heat removal from low-pressure heavy liquid metal on the primary side to the high-pressure water/steam on the secondary side.

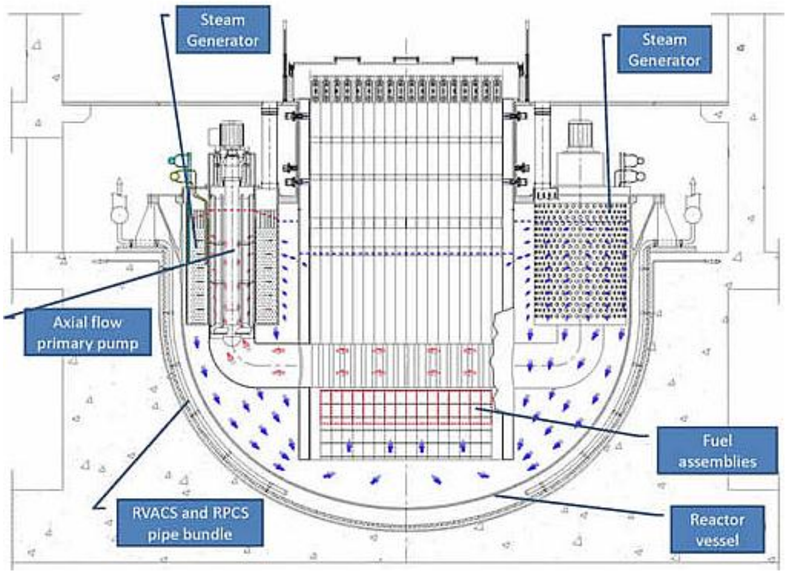


**Figure 1: ELSY reactor reference configuration [6].**

## 1. General approach

A commercial CFD code Star-CCM+ version 5.06.007 [7] is used for modelling of coolant flow field and bubble transport. We are considering the steady state liquid lead flow in the primary system of the ELSY design at nominal full power operation conditions.

The consequences of SGT leakage are studied by injecting bubbles with different diameters into the steam generator region. Bubbles are modelled as Lagrangian tracers. Bubble transport to the core region is contingent upon the balance between the gravity and hydrodynamic drag forces. To account for the effects of fluctuating turbulent velocity field on the trajectories of the bubbles, a turbulent dispersion model, which employs so-called random-walk technique, is employed. A fraction of the bubbles that can reach the core region is calculated by counting the number of bubbles at the core inlet and relating this number to the total number of released bubbles. Similar approach is used to determine the fraction of bubbles that can accumulate in the primary coolant system. We vary the size of the bubbles and location of bubble injection inside the SG to identify the most dangerous bubble size and positions of the leak. The influence of epistemic uncertainty in the correlations for bubble drag in liquid lead is addressed by comparing the probabilities of bubble transport to the core obtained with different correlations.

Liquid lead thermo-physical properties were defined in Star-CCM+ according to the recommended correlations [8]. All the values are calculated (Table 1) based on reference temperature of 750 K (476.85 °C), which is in the range of operating temperatures of coolant in ELSY design (core inlet and outlet temperatures 400 °C and 480 °C, respectively).

**Table 1: Thermo-physical properties of liquid lead at reference temperature.**

| Parameter | Value | Parameter | Value |
|---|---|---|---|
| $T_{ref}$(K) | 750.00 | $T_{boil}$ (K) | 2016.00 |
| Density (kg/m$^3$) | 10 471.2 | $P_{sat}$ (Pa) | $8.46\cdot10^{-4}$ |
| Thermal expansion coefficient (1/K) | $1.14\cdot10^{-4}$ | $T_{sat}$ (K) | 2016.00 |
| Specific heat (J/kg·K) | 145.5 | $Q_{vaporization}$ (J/kg) | 858 200 |
| Mol. viscosity (N·s/m$^2$) | 0.00124 | Surface tension (N/m) | 0.43425 |
| Therm. cond. (W/m·K) | 17.45 | Mol. weight (g/mol) | 207.2 |
| $T_{critical}$ (K) | 4870 | Speed of sound (m/s) | 1 737.97 |
| $P_{critical}$ (MPa) | 100 | | |

## 2. Selection of the bubble drag coefficient

The balance between drag and gravity forces defines the terminal rise velocity of a bubble in lead. Bubble will be dragged down by coolant flow if terminal rise velocity of a bubble will be smaller than local downward velocity of the coolant. Therefore bubble drag coefficient is one of the most important factors that define possibility of bubble transport to the core region. In this section, we discuss selection of a correlation for a steam bubble drag coefficient. For that purpose, terminal rise velocity of a steam bubble in steady liquid lead column is calculated with different drag correlations. Then we compare predicted velocity with available experimental data on a terminal rise velocity of a bubble in heavy liquid metals.

### 2.1 Modelling of bubble motion in lead

Motion of a bubble in liquid and its terminal rise velocity have been studied extensively in the past (e.g. see reviews [9], [10]). Bubble motion dynamics can be affected by many factors (such as temperature, viscosity, pressure, purity). Therefore, prediction of terminal rise velocity is not a trivial task, especially taking into account a non-linear behaviour of drag coefficient, which dependents on the size and the shape of the bubbles. Three different regions can be defined for bubble drag based on equivalent bubble diameter [10]:

- Viscosity-dominated region – very low Reynolds number; bubbles behave like rigid spheres; viscosity force determines the motion; and terminal rise velocity increases with diameter (sometimes also called Stokes region).
- Surface tension-dominated region – bubble shapes are deformed; both, surface tension and inertia determine terminal rise velocity, which can increase, decrease or stay constant with increasing bubble diameter.
- Inertia-dominated region – bubbles are spherical cap shaped; motion is dominated by inertial forces (buoyancy driven); velocity increases with diameter until flattens out to a stable level.

In this work, we use Lagrangian model for bubble transport in a continuum flow field of liquid lead. Steam inside the bubble was assumed to be incompressible and bubble size was not a function of local pressure. Density and viscosity of the bubble gas was assumed equal to water vapour density at 100 °C under atmospheric pressure.

The actual size distribution of the bubbles in case of SG tube leak is an uncertain parameter that depends, among other factors, on the crack morphology (e.g. [2], [9]). In this work, we are considering range of bubble sizes from 0.2 mm to 10 mm. This range of bubble sizes was observed in experiments performed air injection into water with different sizes and geometries of the orifice [11] and also in experiments with water injection into lead [12].

We use four different drag coefficient correlations in the analysis. Firstly, the Schiller-Naumann correlation, which is suitable for spherical, rigid particles (as it is defined in [7]):

$$C_D = \begin{cases} \frac{24}{Re_b}\left(1 + 0.15 Re_b^{0.687}\right); \ 0 < Re_b < 1000 \\ 0.44; \ Re_b > 1000 \end{cases} \tag{1}$$

The dispersed phase (bubble) Reynolds number is defined as:

$$Re_b = \frac{\rho_c |v_r| l}{\mu_c} \tag{2}$$

where $\rho_c$ and $\mu_c$ are the density and the dynamic viscosity of the continuous phase (lead) respectively, $v_r$ is the relative velocity between the bubble and lead, and $l$ is spherical bubble diameter.

Secondly, Schiller-Naumann coefficient with modification in the low Reynolds number region according to Stokes law was used [9]:

$$C_D = \begin{cases} \frac{24}{Re_b}\frac{2 + 3\frac{\mu_d}{\mu_c}}{3 + 3\frac{\mu_d}{\mu_c}} \\ \frac{24}{Re_b}\left(1 + 0.15 Re_b^{0.687}\right); \ 0 < Re_b < 1000 \\ 0.44; \ Re_b > 1000 \end{cases} \tag{3}$$

where $\mu_d$ is the dynamic viscosity of the dispersed phase (steam bubble).

Thirdly, a correlation proposed by Rodrigue [13]:

$$C_D = \frac{16}{Re_b}\begin{bmatrix} (0.5 + 32\Theta + 0.5\sqrt{1 + 128\Theta})^{1/3} + \\ (0.5 + 32\Theta - 0.5\sqrt{1 + 128\Theta})^{1/3} + \\ 0.036\left(\frac{128}{3}\right)^{1/9} Re^{8/9} Mo^{1/9} \end{bmatrix}^{9/4} \tag{4}$$

where $\Theta = (0.018)^3 \left(\frac{2}{3}\right)^{1/3} Re^{8/3} Mo^{1/3}$, $Mo = \frac{g\,\mu_c^4}{\rho_c\,\sigma^3}$ is Morton number. According to Rodrigue, the correlation is applicable for a wide range of bubble sizes and various viscous liquids.

Fourth, correlation used in this work was developed by Tomiyama et al. [14]:

$$C_D = max\left\{min\left[\frac{16}{Re_b}(1+0.15Re_b^{0.687}), \frac{48}{Re_b}\right], \frac{8}{3}\frac{Eo}{Eo+4}\right\} \tag{5}$$

where $Eo = \frac{\Delta\rho\, g\, l^2}{\sigma}$ is Eötvös number, which, together with Morton number, defines the shape of a bubble moving in surrounding fluid. This general correlation fits well with available experimental data.

## 2.2 Modelling of bubble motion in a liquid lead column

For the task of validation of bubble drag correlation, we study bubble rise velocity in a lead column of 0.5 m x 0.5 m x 5 m. The column contains 23,826 polyhedral cells with a characteristic size of about 5-7 cm. The top and the bottom surfaces of the column were defined as walls. The sidewalls of the column were defined as symmetry planes with "rebound" option for the bubbles.

Lead flow field is described as continuous phase whose governing equations are expressed in Eulerian frame of reference. The constant density and segregated flow (and energy) solvers were used as appropriate for incompressible flows [7]. Steady stagnant lead at temperature of 450 °C was used in all cases.

In a reactor simulation, it is important to account for the effect of turbulent dispersion of the bubbles. Without the effect of turbulence, the bubbles will always follow the same streamline, which is physically unreasonable. So-called random-walk model is employed to simulate the effect of fluctuating velocity field on bubble trajectories. A bubble is assumed to be affected by a sequence of eddies as it travels through the turbulent flow field. Every eddy causes a local disturbance to the Reynolds–averaged velocity field

$$v = \bar{v} + v' \tag{6}$$

where $\bar{v}$ is the local Re-averaged velocity and $v'$is the eddy velocity fluctuation. The magnitude of the fluctuation is random at each time instant and has normal (Gaussian) distribution with zero mean value and a standard deviation given by eddy velocity scale, which is described by the following formula

$$u_e = \frac{l_t}{\tau_t}\sqrt{\frac{2}{3}} = \sqrt{\frac{2}{3}k} \tag{7}$$

where $l_t$ and $\tau_t$ are the length-scale and time-scale of the turbulence and $k$ is turbulent kinetic energy provided by the turbulence model (k-epsilon used in this case) [7]. We considered uniform turbulence in stagnant flow with constant value of turbulent kinetic energy 0.1 J, which corresponds to eddy velocity fluctuation of about 0.25 m/s. One can envisage a situation when a steady pool is stirred to introduce eddies with constant energy while the averaged flow is zero.

Terminal velocity of rising bubble in laminar stagnant column was determined as the bubble velocity at the column outlet. In case of turbulent stagnant flow the terminal rise velocity was calculated based on the column height and residence time of the particles.

## 2.3 Results

Since there is no available experimental data on bubble terminal rise velocity in lead, the simulation results were compared to Stokes law that predicts velocity for small, spherical shape bubbles and to Mendelson's equation that predicts velocities in surface tension- and inertia-dominated regimes

[15]. Comparison of Stokes law and Mendelson equation with experimental data for bubble terminal rise velocity in mercury obtained by Mori et al. [16] is shown in Figure 2. As it can be seen, the bubble velocity is predicted reasonably well by Mendelson's equation in the surface tension dominated regime. Small bubbles are expected to behave as solid spheres and their terminal velocity should be described by Stokes law. However, there is an uncertainty in the transition from surface tension-inertia dominated region to Stokes region.

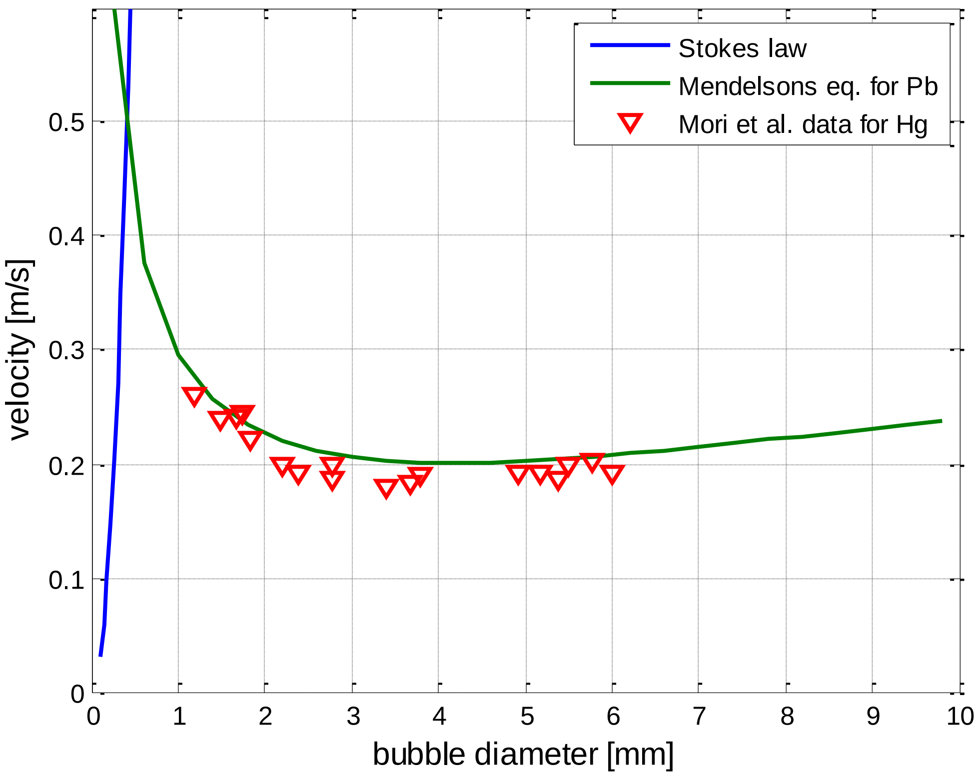


**Figure 2: Bubble terminal velocity vs. bubble diameter. Analytical predictions by Stokes and Mendelson laws. Experimental data for mercury.**

First calculations were performed without activating turbulent dispersion model for the bubbles. Figure 3 presents the terminal rise velocities obtained using different drag correlations described in the previous section. It can be seen that Schiller-Naumann correlation is applicable only for very small bubbles, which behave as rigid spheres. The modified Schiller-Naumann correlation does not improve the results. Rodrigue's correlation shows a better agreement than Schiller-Naumann, but is still deficient in capturing the peak on the curve of terminal velocity. Tomiyama's drag correlation, which aims to match the whole drag curve, provides the best agreement with the Stokes solution and Mendelson equation for bubble rise velocities. Therefore, Tomiyama's correlation was used for the study of bubble transport in reactor conditions.

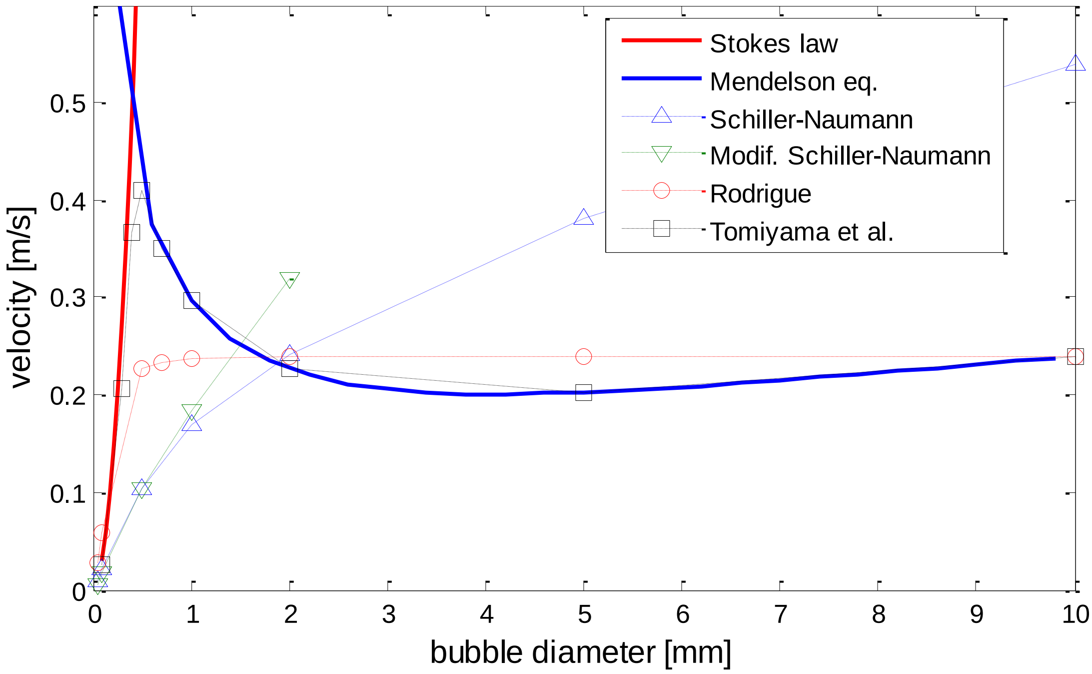


**Figure 3: Bubble terminal rise velocities calculated with different drag coefficient correlations.**

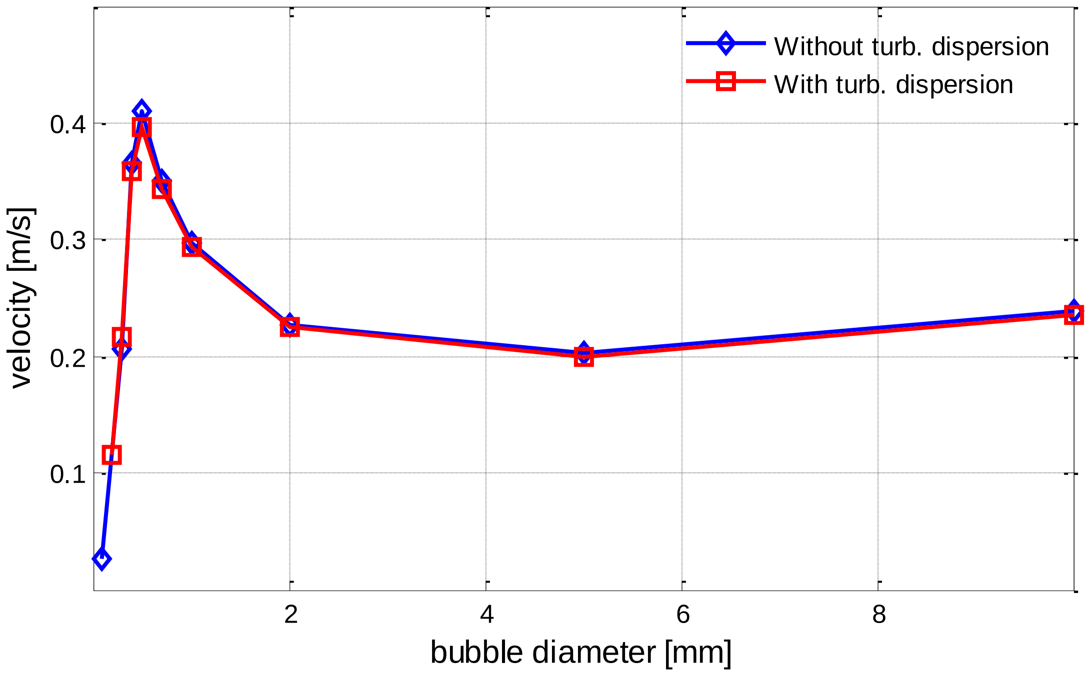


**Figure 4: Bubble terminal rise velocity with and without modeling of turbulent dispersion.**

A comparison between the results obtained with and without turbulent dispersion modelling was done for Tomiyama's correlation. As it appears in Figure 4, a difference between averaged terminal rise velocity of a bubble in stagnant laminar and in turbulent lead column is negligible as it is expected.

## 3. Prediction of bubble transport to the core region

In this section we address possibility of bubble transport from the steam generator to the core region in the ELSY design at nominal operation conditions. First we resolve the averaged steady state flow at full power operation in a realistic configuration of the primary system. Then we study behavior of individual bubbles in the flow field with Lagrangian approach, taking into account dispersion of the bubbles by turbulent vortices. The probability that a bubble of certain size can reach the core region and then stay in the primary coolant system is assessed for the bubbles released at different locations in the SG.

## 3.1 Modelling of primary coolant flow

The simulation domain represents 1/8th slice of the ELSY reactor vessel, comprising one SG with hot leg and a pump and a slice of the core region with corresponding sections of the hot/cold plenum and downcomer.

### 3.1.1 Physical models and numerical methods

The coupled implicit solver was used for mass, momentum and energy equations. Flow was modelled as incompressible whereas gravity option incorporates the Boussinesq approximation in the momentum equation to model the buoyancy due to thermal expansion of the coolant. The RANS realizable $k - \varepsilon$ model with two-layer all-y+ formulation [7] was chosen for simulation of the turbulence effects.

### 3.1.2 Design parameters for nominal operation and numerical boundary conditions

The nominal operational parameters for the steady state flow are following:

- Mass flow 16.05 ton/s/SG
- Core inlet temperature 400 °C [5]
- Core outlet temperature 480 °C [5]
- Core pressure drop 0.9 bar [5],[17]
- Steam generator pressure drop 0.3 bar [17],[18]
- Total primary pressure drop 1.4 bar [5]

Parameters presented above were used to determine a set of boundary conditions, uniformly distributed heat source term in the core region, heat sink term in the steam generator region, and momentum source term in the pump region (see Figure 5 and Table 2).

**Table 2: Defined source terms per region.**

| Region | Quadratic resistance coefficient [kg/m⁴] | Heat source/sink [W/m³] | Porosity | Momentum source [N/m³] |
|---|---|---|---|---|
| **Core** | 112 635 | $9.2 \cdot 10^{7}$ | 0.5 | - |
| **Steam generator** | $1.25 \cdot 10^{7}$ | $\frac{T-335°C}{145°C} \cdot \frac{-187.5MW}{V_{SG}}$ | 0.65 | - |
| **Upper/lower plenum** | 112 635 | - | 0.6 | - |
| **Pump** | 74 093 | - | 0.9 | 540 000 |
| **Shielding** | $2.2527 \cdot 10^{7}$ | - | 0.9 | - |

Core, SG, upper/lower plena and shielding regions were modeled as porous media. A source of momentum in the pump was adjusted along with quadratic resistance coefficients for the porous media regions, to obtain mass flow rate according to design. Heat sink expression, as described in Table 2, assured that the lead temperature at the SG inlet is 480°C at nominal heat removal rate. In total, 9 regions were defined in the simulation domain. All the solid boundaries in the design are modelled as adiabatic, no-slip walls. Vertical left and right sides of the simulation domain are defined as symmetry planes. Free surfaces (hot and cold, see Figure 9) are defined as adiabatic, slip walls.

### 3.1.3 Mesh

The mesh was created with Star-CCM+ internal mesher based on the geometry extracted as boundary surface from initial volume mesh, which was originally created by our colleague Dr. Johan Carlsson with Pointwise Gridgen [19]. The mesh used in the calculation consists of 679 480 polyhedral cells. Target characteristic size of a cell in the domain was 0.07 m. We used 5 layers of prism cells for the modelling of boundary layers on the solid walls. The total thickness of the prismatic cell layer was 0.02 m and smallest prism cell height near the wall was 0.0015 m and the wall $y^+$values were mostly below 100. The 3D volume mesh (with distinct regions) and the mesh on a vertical cross-section is shown in Figure 5.

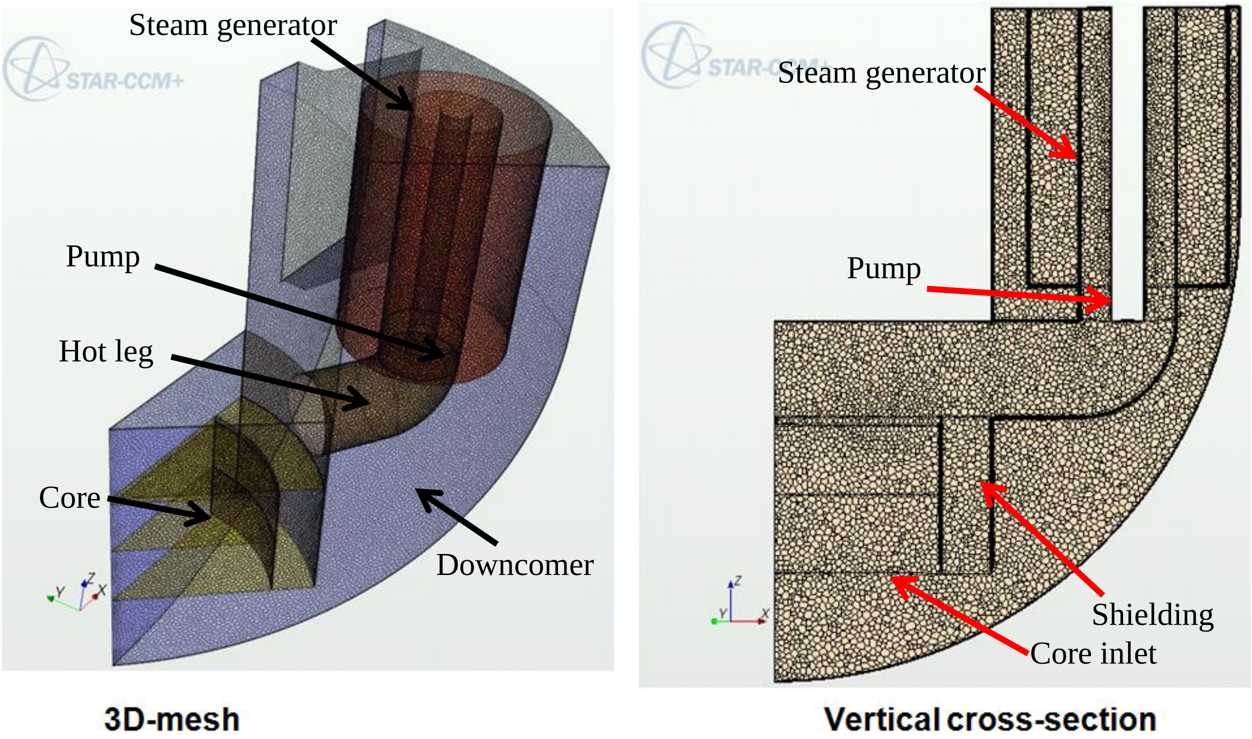


**Figure 5: 3D volume mesh and a vertical cross-section of it.**

### 3.1.4 Results of primary coolant flow simulation in steady state nominal operation

A satisfactory steady state was achieved at nominal mass flow rate of 16.09 ton/s and area averaged temperatures at core inlet 402.7 °C and core outlet 485.3 °C, which gives an average temperature increase in the core 82.6 °C. Predicted pressure drop in the core was 0.85 bars and 0.29 bars in the SG. Total pressure drop of 1.6 bars was calculated for the whole primary system. Coolant temperature distribution in the vertical cross-section plane is shown in Figure 6. Analysis of the velocity vector field presented in Figure 7 suggests that there is a region near the vessel wall in the downcomer with relatively high downward speed of the coolant flow. As we will show in the next section such flow is capable of dragging steam bubbles from the SG to the core region.

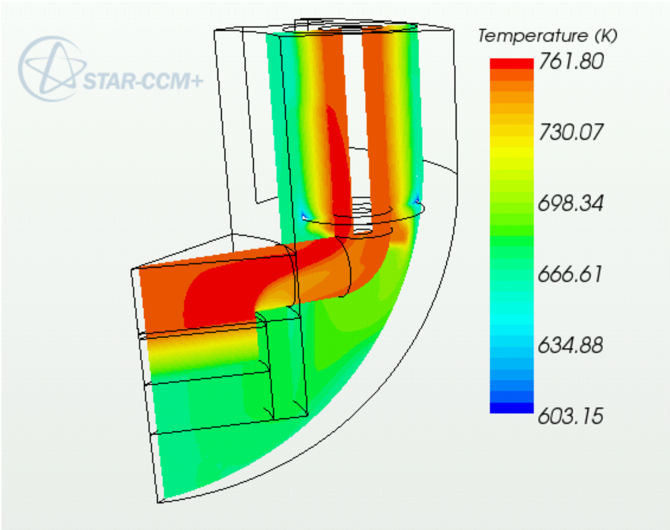


**Figure 6: Temperature field during normal operation.**

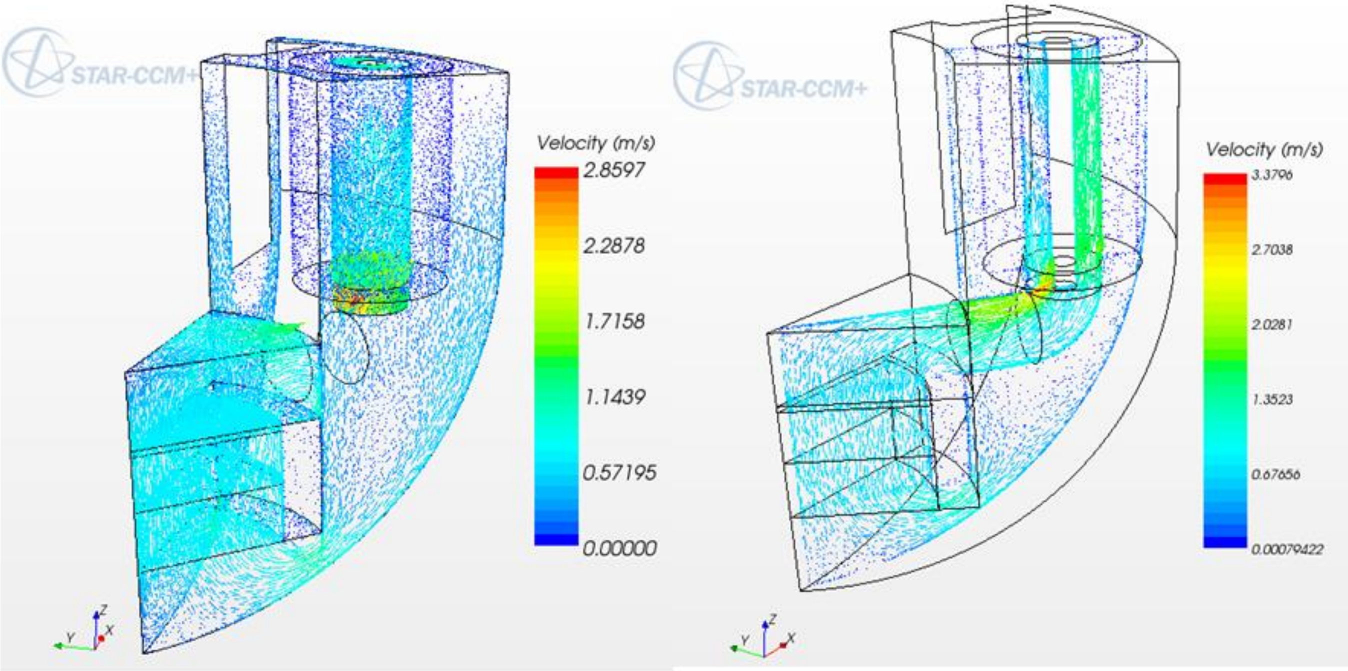


**Figure 7: Velocity profiles in the steady state flow field (3D on the left and 2D vertical cross-section on the right).**

## 3.2 Modelling of steam bubble transport in the primary system

To study the possibility of steam bubble transport to the core region we use Lagrangian model that resolves individual trajectories of the bubbles in turbulent flow field of the primary coolant system. Bubble is assumed to have constant density. Injectors are used in Star-CCM+ to define the location, direction and rate at which the bubbles enter the fluid continuum. Bubbles were injected at three different levels (see Figure 8) in the SG – 5.2 m, 6.87 m and 8.55m from the bottom of the pool (the total depth of the pool is 8.65 m). A point inclusion probability (probability of a point being included in a set of points from which bubbles are injected) is used in Star-CCM+ to control the number of bubble seeds. The point inclusion probability is equal to ratio of the number of seeds to the total number of cells in the seed plane. In the SG region we used several point inclusion probabilities from 0.005 to 1.0 that correspond to the numbers of particle seeds from 24 to 4142. Changes in the results presented below are insignificant if number of seeds is greater than 2500.

"Rebound" conditions were implemented on the solid walls of the primary system and "escape" conditions were used on the free coolant surfaces. Initial velocity of a bubble was set to 0 m/s and flow rate of a bubble from one seed point was selected as one bubble per second. Behaviour of the bubble with diameters of 0.2, 0.4, 0.5, 1.0, 2.0, 4.0 and 6.0 mm was studied. To investigate the effect of the bubble drag coefficient, both, Tomiyama and Schiller-Naumann correlations were used in the analysis.

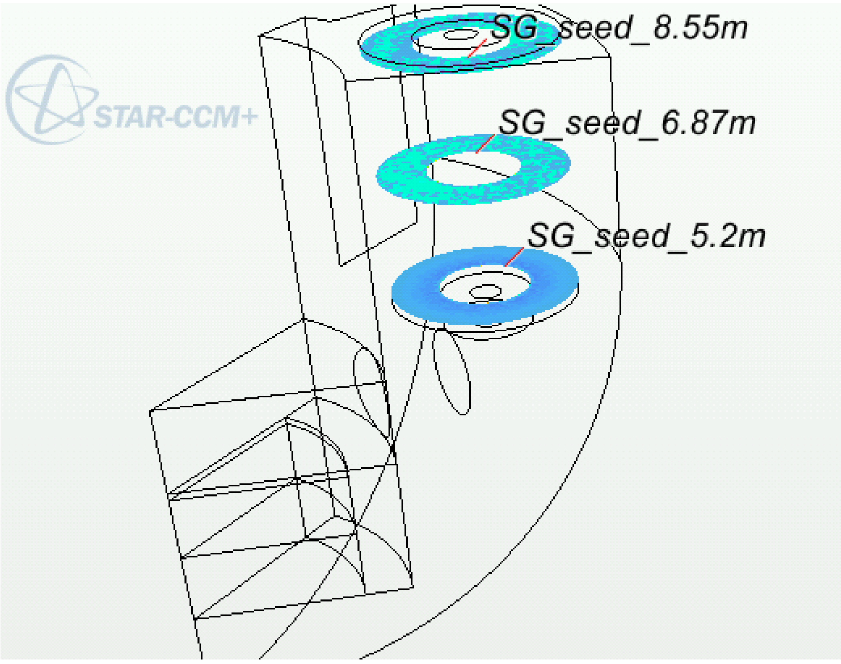


**Figure 8: Locations of the planes used as bubble injectors.**

### 3.3 Estimation of a fraction of bubbles that reach the core

Here we describe a method for assessment of the probabilities that a bubble emerging from a leaking steam generator tube can reach the core inlet and then stay circulating in the primary coolant. The following three-step method is used in assessment of void accumulation rate in the core (and in the primary system). Bubbles injected through the crack in SGT into the primary coolant flow have generally three possibilities to escape the system (see Figure 9) depending on their size, leak location and coolant flow characteristics:

1. Bubble escapes after injection immediately to the cold free surface above the downcomer and the SG.
2. Bubble is dragged down to the core for the first time and then escapes from the loop to the hot free surface above the core.
3. Bubble stays in the primary coolant flow, travels through the hot leg and pump and reaches the SG again. Then it emerges to the cold free surface.

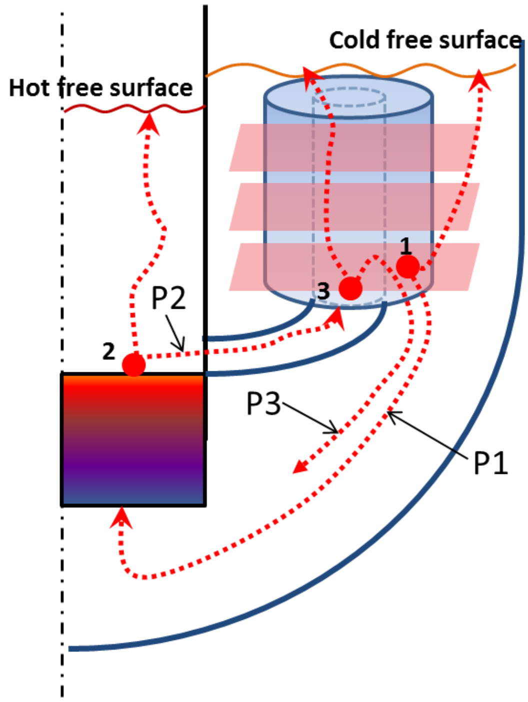


**Figure 9: Different locations of bubble injection (1-3) and respective probabilities that injected bubble can stay in the loop (P1-P3).**

All the bubbles which do not escape from the coolant will be carried by the coolant flow through the primary loop again to the core. In order to assess the consequences of the SGTL and different scenarios of void behaviour in the primary system we need to calculate the probabilities that a bubble will escape from the coolant given the abovementioned three possibilities.

P1 is the probability that a bubble can reach the core after entering the primary coolant flow through the SG tube leak. We calculate this probability by injecting bubbles at one of the three injection levels in the SG and counting the number of the bubbles that reach the core inlet boundary. P2 is the probability that a bubble can reach SG after passing through the core. To estimate the P2, we inject bubbles at the exit of the core and count those that escape to the hot free surface. One minus obtained fraction of the bubbles that escape from the coolant is equal to P2. Finally, P3 is the probability that a bubble stays in the primary loop after passing through the core and the pump. To calculate the P3 we inject bubbles at the exit of the pump and count those that reach the core inlet.

If leak rate and bubble size distribution in case of SGTL are known, one can estimate the total rate of void accumulation in the coolant in the form of the bubbles that are circulating in the primary system:

$$Q_{primary}(t) = Q_{leak}(t) \sum_{i=1,N} f_{d_i} \cdot P_{1_{d_i}} \cdot P_{2_{d_i}} \cdot P_{3_{d_i}} \quad (8)$$

where $Q_{leak}$ is volumetric leak rate [litres/day], $f_{d_i}, P_{1_{d_i}}, P_{2_{d_i}}, P_{3_{d_i}}$ are volume fraction and respective probabilities for a bubble with size $d_i$, and $N$ is the number of bubbles sizes considered in the bubble size distribution.

It is also interesting to estimate the void accumulation rate in the core (assuming that all bubbles that reach the core will stuck in the core, e.g. below spacers):

$$Q_{core}(t) = Q_{leak}(t) \sum_{i=1,N} f_{d_i} \cdot P_{1_{d_i}} \quad (9)$$

To estimate the realistic rate of void accumulation in the core one needs to consider the probability that bubble will pass or stuck in the core given detailed geometry of the core internals. This task is beyond the scope of the present work.

# 4. Results and discussion

## 4.1 Injection level 5.2 m

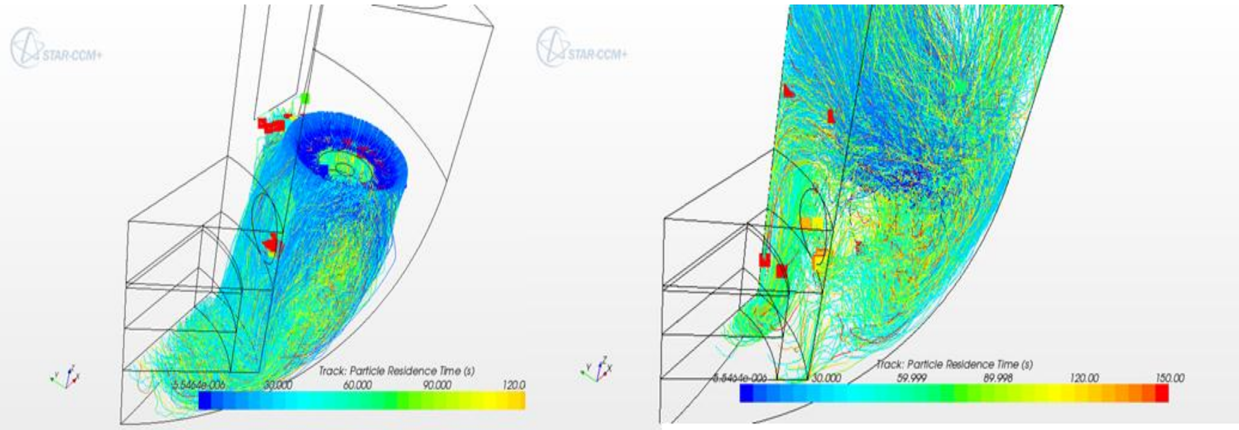


**Figure 10: Trajectories of 0.2 mm (left figure) and 2.0 mm (right) bubbles injected at the level of 5.2 m.**

Examples of the trajectories of bubbles injected at the level of 5.2 m are shown in Figure 10. The probability that a bubble can reach the core (P1) as a function of bubble size is presented in Figure 11. It is clear that there is non-zero probability for bubbles with diameter less than 0.5 mm and bigger than 1.0 mm to reach the core if Tomiyama drag correlation (blue curve) is used. This plot also confirms that Schiller-Naumann drag correlation (red curve) can be used only for very small bubbles. Results obtained with this correlation for bubbles bigger than 0.2 mm can be generally misleading.

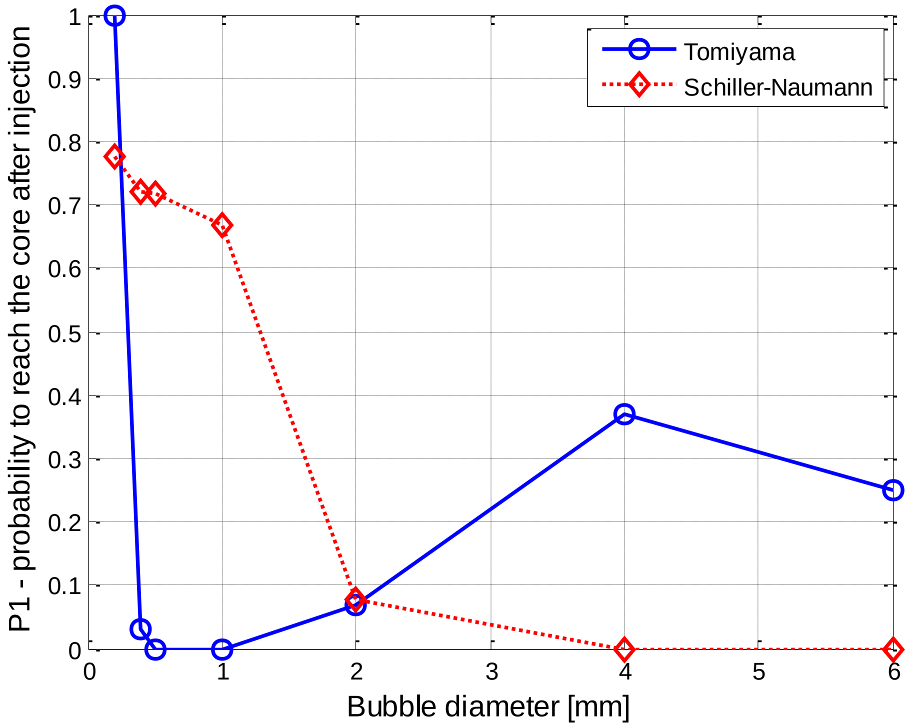


**Figure 11: Fraction of bubbles that reach the core inlet after injection at the level 5.2 m. Results obtained with different correlations for drag coefficients.**

## 4.2 Injection level 6.87 m

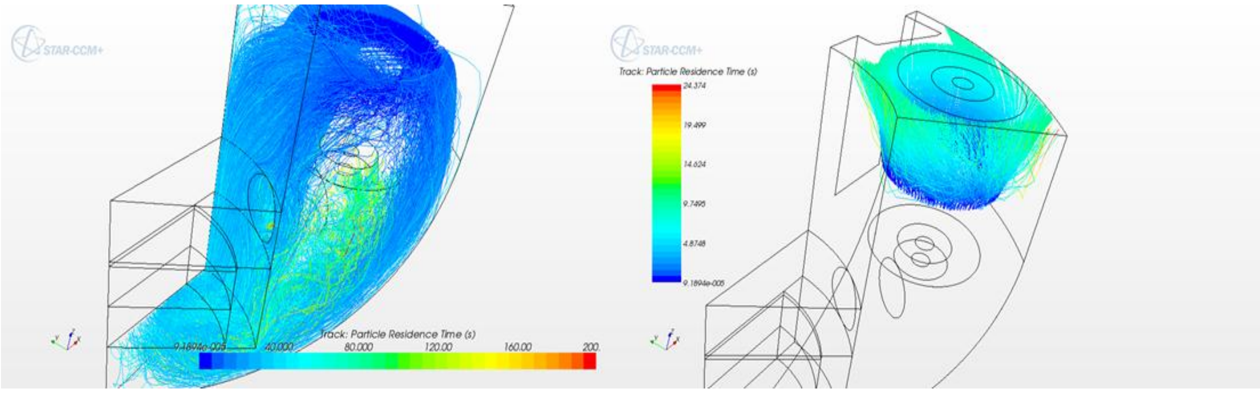


**Figure 12: Trajectories of 0.2 mm (left figure) and 2.0 mm (right) bubbles injected at the level of 6.87 m.**

Figure 12 illustrates the trajectories of bubbles injected at the level of 6.87 m. The probability that a bubble can reach the core (P1) as a function of bubble size is presented in Figure 13. At this injection level both drag correlations show similar tendency, namely that the large bubbles are escaping from the coolant and the smallest bubbles present certain risk of coolant voiding.

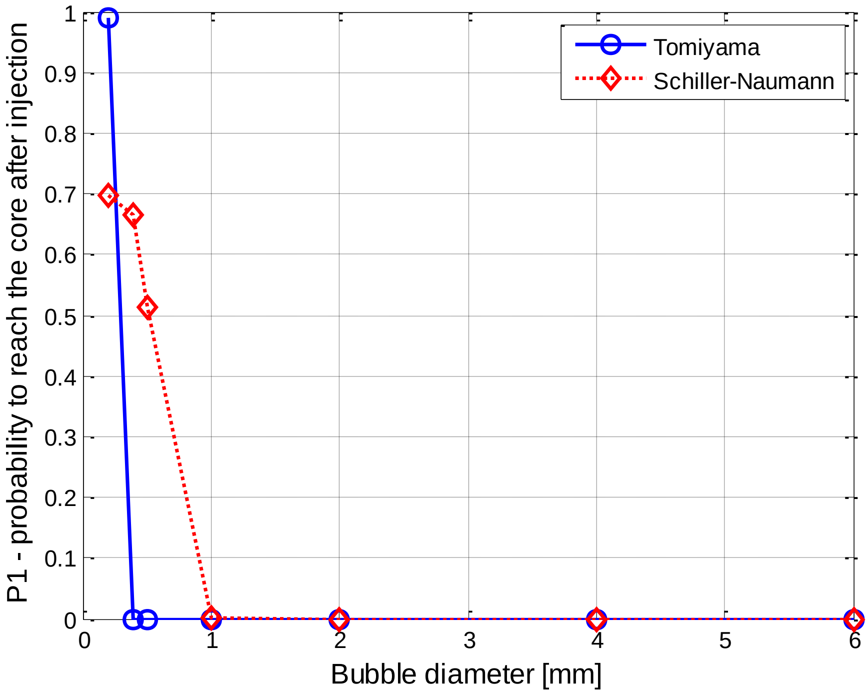


**Figure 13: Fraction of bubbles that reach the core inlet after injection at the level 5.2 m.**

## 4.3 Injection level 8.55 m

All bubbles escape immediately to the cold free surface and there are no bubbles carried to the core if the leak is located at the top part of the SG. An example of the bubble trajectories injected at top location in steam generator is depicted in Figure 14.

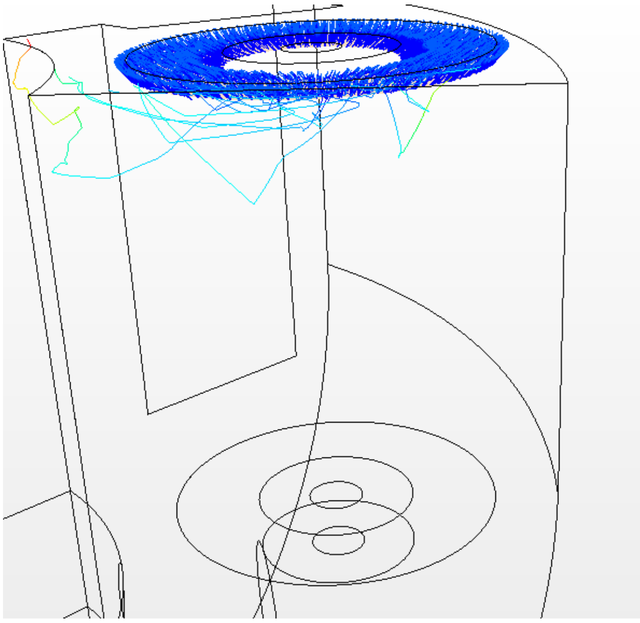

**Figure 14: Trajectories of 0.2 mm bubbles injected at the level of 8.55 m.**

## 4.4 Estimation of probabilities P2 and P3

Probability that a bubble will reach steam generator after passing through the core (P2) is presented in Figure 15. Note that significant fraction of the bubbles (more than 50%) is able to reach the pump. Trajectories of 0.5 mm bubbles can be seen in Figure 16.

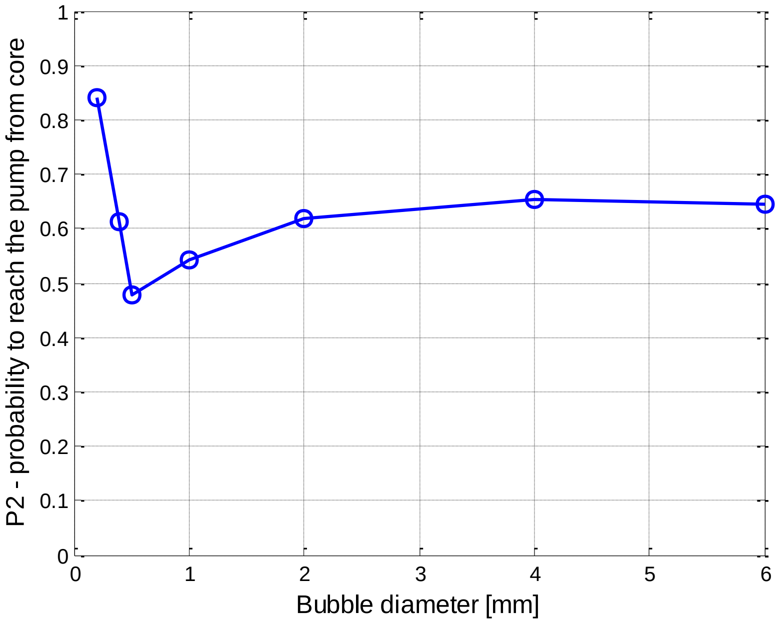


**Figure 15: Probability that a bubble injected at the core outlet can reach the pump.**

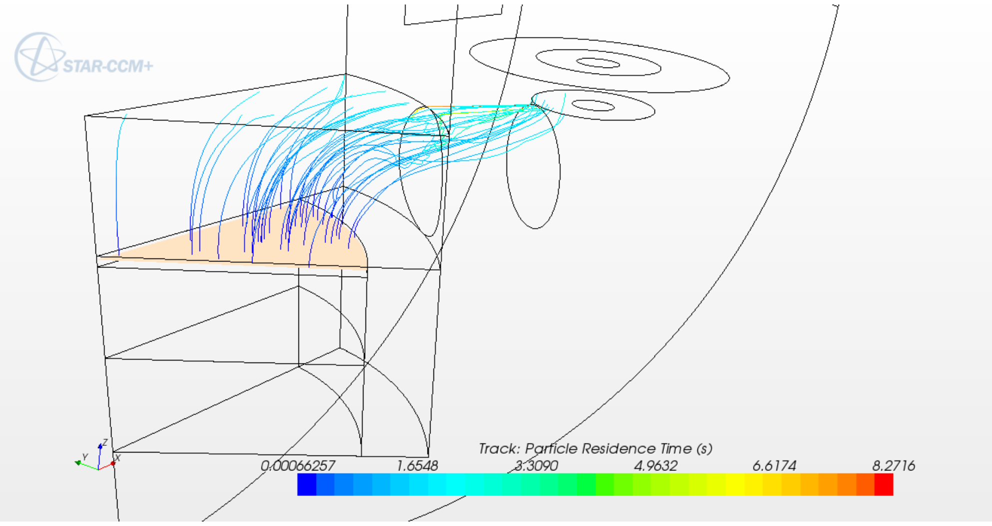


**Figure 16: Trajectories of 0.5 mm bubbles injected at the core outlet.**

Probability that a bubble will reach the core inlet again after passing through the pump (P3) is presented in Figure 17 for different bubble sizes. Trajectories of 0.2 mm bubbles are shown in Figure 18. Results of simulations suggest that only small bubbles (0.2 mm) can reach the core inlet if injected in the pump region.

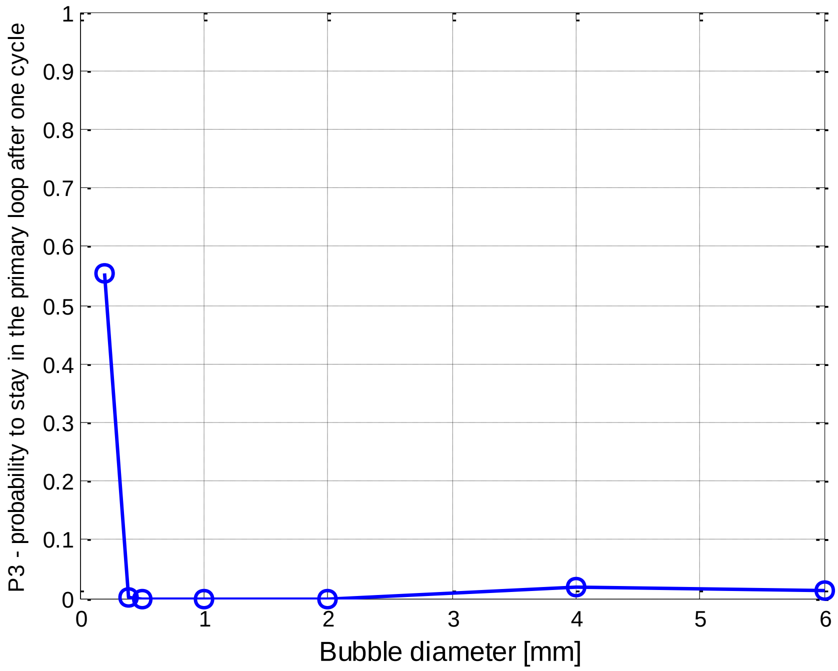


**Figure 17: Probability that a bubble injected at the pump outlet will reach the core inlet.**

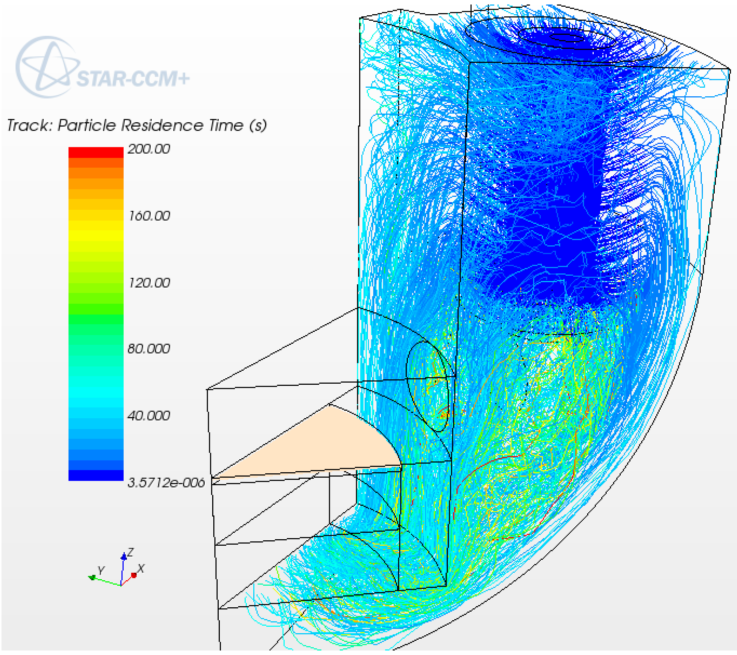


**Figure 18: Trajectories of 0.2 mm bubbles when injected close to the pump outlet.**

## 4.5 Accumulation rates

In this analysis we have used leak flow rates taken from studies by Hwang et al. [3], [20], [21] and the bubble size distribution ranges from Terasaka et al. [22] and Beznosov et al. [12]. We have estimated the accumulation rates in the core and in the primary system.
The results are following:

1. Injection level 5.2 m
   a. Accumulation in the primary system Eq. (8) 0.012 – 0.85 L/day
   b. Transport to the core Eq. (9) 0.09 – 96.44 L/day
2. Injection level 6.87 m
   a. Accumulation in the primary system Eq. (8) 0.01 – 0.02 L/day
   b. Transport to the core Eq. (9) 0.02 – 0.03 L/day
3. Injection level 8.55 m No accumulation

The smaller value in the range of accumulation rates is calculated using leak rate of 7.2 litres per day (few drops per minute), which is typical for the initial stage of the crack development, and size distribution with smaller bubbles[22] The bigger value is calculated based on maximum leak rate of 360 litres per day and size distribution with larger bubbles [12].

## 5. Summary and conclusion

In this paper we consider potential consequences of a steam generator tube leakage in a pool type Lead cooled Fast Reactor design. Primary coolant flow in normal operation conditions and steam bubble transport in the primary coolant loop is simulated with CFD. Bubbles are injected at different locations inside the steam generator volume. Tomiyama’s drag model is selected for simulation of steam bubbles motion in lead. Probabilities that bubbles can reach the core inlet and then stay in the primary loop have been estimated. We found that bubbles with diameters between 0.5 mm and 1 mm, leaking from the bottom part of the SG, are likely to escape from the primary system before they reach the core inlet. The other bubbles can contribute to voiding of primary system. If the leakage is located in the middle of the SG, only bubbles with diameter less than 0.4 mm can reach the core. Bubbles appearing in the top part of the SG will escape from the primary loop regardless of their diameter.

The main outcome of this study is that there is a possibility that steam bubbles can be dragged to the core in significant amounts. The extent to which it happens depends on the bubble size distribution, leak flow rate and injection location. We show that void accumulation rate in the primary system can be up to about 0.9 litres per day. If all bubbles assumed to get stuck in the core, then the accumulation rate in the core can be up to 96 litres per day. It is also not excluded that the bubbles can accumulate in some stagnation zones near the core inlet and then enter to the core in a form of a big bubble threatening core integrity. The finding about considerable fraction of the bubbles that can reach the core inlet in nominal operation conditions as a result of SGTL helps to infer that adequate preventive and mitigative measures are necessary in the design of pool-type LFR systems with positive void reactivity coefficient.

## 6. Acknowledgment

The work was performed in the framework of EC ELSY and LEADER projects. Authors are grateful to Dr. Johan Carlsson from JRC for providing the geometry of the ELSY primary coolant system used in the simulations.

## 7. References

[1] B.W. Spencer, "The Rush to Heavy Liquid Metal Reactor Coolants – Gimmick or Reasoned", Proceedings of ICONE-8, 8th International Conference on Nuclear Engineering, April 2-6, 2000, Baltimore, MD USA.

[2] P. Kudinov and T.N. Dinh, "Evaluation approach and case set-up for simulation of consequences of the SGTR event", Division of Nuclear Power Safety, Royal Institute of Technology, Stockholm, 2010.

[3] S.S. Hwang, H.P. Kim, J.S. Kim, K.E. Kasza, J. Park, and W.J. Schack, "Leak behavior of SCC degraded steam generator tubings of nuclear power plant," *Nuclear Engineering and Design*, **235**, 2005, 2477-2484.

[4] EPRI Technical Report. "PWR Primary-To-Secondary Leak Guidelines – Revision 2," EPRI, Palo Alto, CA: TR-104788-R2. 2000.

[5] L. Cinotti, "Reactor Assembly Preliminary Configuration", Del Fungo Giera Energia S.p.A, 2008, ELSY DOC 08 049.

[6] The Generation IV International Forum. [Online] [Cited: 16 March 2011.] http://www.gen-4.org.

[7] CD-Adapco, *Star-CCM+ User Guide version 5.02.*

[8] "Handbook on lead-bismuth eutectic alloy and lead properties, materials compatibility, thermal-hydraulics and technologies," OECD NEA, No. 6195 2007.

[9] A. A. Kulkarni and J. B. Joshi, "Bubble formation and bubble rise velocity in gas-liquid systems: a review", *Ind. Eng. Chem. Res.*, Vol. 44, 2005, 5873-5931.

[10] G. Q. Yang, Bing Du, and L. S. Fan, "Bubble formation and dynamics in gas-liquid-solid fluidization – a review", *Chem. Eng. Sci.*, Vol. 62, 2007, 2-27.

[11] E. Krepper, D. Lucas, and H.-M. Prasser, "On the modelling of bubbly flow in vertical pipes", *Nucl. Eng. Des.*, Vol. 235, 2005, 597-611.

[12] A. V. Beznosov, S. S. Pinaev, D. V. Davydov, A. A. Molodtsov, T. A. Bokova, P. N. Martynov and V. I. Rachkov, "Experimental studies of the characteristics of contact heat exchange between lead coolant and the working body", *Atomic Energy*, Vol. 98, Issue 3, 2005.

[13] D. Rodrigue, "A simple correlation for gas bubbles rising in power-law fluids", *Can. J. Chem. Eng.*, Vol. 80, Issue 2, 2002, 289.

[14] A. Tomiyama, I. Kataoka, I. Zun, and T. Sakaguchi, "Drag coefficients of single bubbles under normal and microgravity conditions", *JSME Int. J. Ser. D*, Vol. 41, Issue 2, 1998, 472.

[15] H. D. Mendelson, "The prediction of bubble terminal velocities from wave theory", *A.I.Ch.E. Journal*, 13, 1967, 250.

[16] Y. Mori, K. Hijikata, and K. Kuriyama, "Experimental study of bubble motion in mercury with and without a magnetic field", *J. Heat Transfer (Trans. ASME)*, Vol. 99, 1977, 404-410.

[17] M. Böttcher, "CFD analysis of decay heat removal scenarios of the lead cooled ELSY reactor", Benchmarking of CFD Codes for Application to Nuclear Reactor Safety (CFD4NRS-3), Bethesda, Md., September 14-16, 2010.

[18] A. Onea, M. Böttcher, and D. Struwe, "Lead pressure loss in the heat exchanger of the ELSY fast lead-cooled reactor by CFD approach", Benchmarking of CFD Codes for Application to Nuclear Reactor Safety (CFD4NRS-3), Bethesda, Md., September 14-16, 2010.

[19] J. Carlsson, "Steam generator tube leakage calculations on the ELSY design," EC JRC, Inst. for Energy, 2009.

[20] S. S. Hwang, H. P. Kim, and J. S. Kim, "Evaluation of the burst characteristics for axial notches on SG tubings, " *Nuclear Engineering and Design*, Vol. 232, 2004, 139-143.

[21] S. S. Hwang, C. Namgung, M. K. Jung, H. P. Kim, and J. Kim, "Rupture pressure of wear degraded alloy 600 steam generators tubings, " Journal of *Nuclear Materials*, Vol. 373, 2008, 71-74.

[22] K. Terasaka, Y. Sasada, D. Kobayashi, and S. Fuijoka, "Submilli-bubble dispersion from a slit orifice into water, " *Journal of Chemical Engineering*, Vol. 44, Issue 3, 2005.